

Comparison of Low-Redshift Lyman- α Forest Observations to Hydrodynamical Simulations with Dark Photon Dark Matter

James S. Bolton^{1,*}, Andrea Caputo^{2,3,†}, Hongwan Liu^{4,5,‡} and Matteo Viel^{6,7,8,9,§}

¹*School of Physics and Astronomy, University of Nottingham, University Park, Nottingham, NG7 2RD, United Kingdom*

²*School of Physics and Astronomy, Tel-Aviv University, Tel-Aviv 69978, Israel*

³*Department of Particle Physics and Astrophysics, Weizmann Institute of Science, Rehovot 7610001, Israel*

⁴*Center for Cosmology and Particle Physics, Department of Physics, New York University, New York, New York 10003, USA*

⁵*Department of Physics, Princeton University, Princeton, New Jersey, 08544, USA*

⁶*SISSA—International School for Advanced Studies, Via Bonomea 265, I-34136 Trieste, Italy*

⁷*IFPU, Institute for Fundamental Physics of the Universe, Via Beirut 2, I-34151 Trieste, Italy*

⁸*INFN, Sezione di Trieste, Via Valerio 2, I-34127 Trieste, Italy*

⁹*INAF—Osservatorio Astronomico di Trieste, Via G. B. Tiepolo 11, I-34143 Trieste, Italy*



(Received 6 July 2022; revised 13 September 2022; accepted 13 October 2022; published 18 November 2022)

Recent work has suggested that an additional $\lesssim 6.9$ eV per baryon of heating in the intergalactic medium is needed to reconcile hydrodynamical simulations with Lyman- α forest absorption line widths at redshift $z \simeq 0.1$. Resonant conversion of dark photon dark matter into low frequency photons is a viable source of such heating. We perform the first hydrodynamical simulations including dark photon heating and show that dark photons with mass $m_{A'} \sim 8 \times 10^{-14}$ eV c^{-2} and kinetic mixing $\epsilon \sim 5 \times 10^{-15}$ can alleviate the heating excess. A prediction of this model is a nonstandard thermal history for underdense gas at $z \gtrsim 3$.

DOI: [10.1103/PhysRevLett.129.211102](https://doi.org/10.1103/PhysRevLett.129.211102)

Introduction.—The Lyman- α forest, a series of absorption features that arise from the distribution of intergalactic gas, is a powerful tool for investigating the properties of dark matter (DM). The absorption is typically observed in the spectra of distant, luminous quasars, where resonant scattering along the line of sight occurs as photons redshift into the rest frame Ly- α ($n = 1 \rightarrow 2$) transition of intervening neutral hydrogen [1]. The 1D power spectrum of the Ly- α forest transmitted flux is an excellent tracer of the underlying DM distribution on scales ~ 0.5 –50 comoving Mpc, and has been routinely used to place tight constraints on warm DM [2–6], fuzzy DM [7–10], as well as primordial black hole (PBH) DM [11].

In addition, the Ly- α forest is also a calorimeter; the widths of the absorption lines are sensitive to the temperature of intergalactic hydrogen. Canonically, it is assumed this temperature is set by photoelectric heating by the integrated ultraviolet (UV) emission from stars and quasars [12,13], and indeed, this paradigm provides an excellent match to the observed properties of the Ly- α forest at redshift $z > 2$ [14,15]. Nevertheless, the thermal state of the intergalactic medium (IGM) can also be used to constrain a variety of other possibilities, such as heating by decaying

and annihilating DM [16–27], light PBHs [25], DM-baryon interactions [28], and ultralight dark photon DM [29–32].

The physics behind Ly- α forest temperature measurements is straightforward. The hydrogen atoms in the IGM will in general not be at rest, but will undergo thermal motion described by a Maxwellian velocity distribution, leading to a line width $\Delta\nu = \nu_\alpha (b_{\text{th}}^2 + b_{\text{nth}}^2)^{1/2}/c$, where c is the speed of light, ν_α is the resonance line frequency, $b_{\text{th}} = (2k_B T/m_H)^{1/2}$ is the Doppler parameter due to thermal motion, m_H is the hydrogen atom mass, T is the temperature of the IGM, and k_B is Boltzmann's constant. Here, b_{nth} accounts for any additional, nonthermal line broadening, including, smoothing of the absorbing structures by gas pressure, small-scale turbulence, peculiar motion or expansion with the Hubble flow. b_{nth} is in general nonzero for all but the narrowest Ly- α lines. Hence, given a forward model for b_{nth} , typically provided by cosmological hydrodynamical simulations, a determination of the Ly- α spectral width—either by directly measuring Doppler parameters or using another statistic that is sensitive to the thermal broadening kernel—allows a measurement of the IGM temperature [33–41].

Thus far, all the calorimetric constraints on new physics from the Ly- α forest have relied on observations at redshifts $z \gtrsim 2$. In this Letter, we pioneer the use of low-redshift ($z \simeq 0.1$) Ly- α forest observations for this purpose. Three independent studies [42–44] have now highlighted a discrepancy between the widths of Ly- α forest absorption lines measured from Hubble Space Telescope/Cosmic

Published by the American Physical Society under the terms of the [Creative Commons Attribution 4.0 International license](https://creativecommons.org/licenses/by/4.0/). Further distribution of this work must maintain attribution to the author(s) and the published article's title, journal citation, and DOI. Funded by SCOAP³.

Origins Spectrograph (COS) data at $z \simeq 0.1$ [45,46] and the predictions from detailed cosmological hydrodynamical simulations. The simulated linewidths are always too narrow compared to the observations. Appealing to enhanced photoelectric heating alone is not a viable solution, as the integrated UV background would require an unphysically hard spectrum [47]. This implies there is a noncanonical heating process in the IGM neglected in the simulations, such that an additional $\lesssim 6.9$ eV per baryon is deposited into typical Ly- α forest absorbers by $z = 0.1$, and/or the nonthermal line broadening has been underestimated [47]. Additional turbulence below the simulation resolution limit is possible [44,48,49], although current models have line widths that become narrower, rather than broader, with increasing resolution. Here, we instead explore the role of additional heating, and suggest that ultralight dark photon DM with a small mixing with the standard model (SM) photon provides an intriguing solution to the linewidth discrepancy. Dark photons can undergo resonant conversions into SM photons, which are subsequently absorbed by the IGM. The condition for resonant conversion is set by the dark photon mass and the local electron density, allowing dark photons to naturally explain the low-redshift Ly- α forest data without altering the established agreement with IGM temperature measurements at $z > 2$.

Dark photon dark matter.—The dark photon A' is a minimal and well-motivated extension of the SM which kinetically mixes with the ordinary photon, γ [50–57]. Ultralight dark photons are also an attractive cold DM candidate, with several early-universe production mechanisms that have been studied extensively in the literature that are capable of producing A' nonrelativistically [58–69]; its perturbations are therefore expected to be well described by the standard Λ CDM matter power spectrum. The photon-dark photon Lagrangian reads

$$\mathcal{L}_{\gamma A'} = -\frac{1}{4}F_{\mu\nu}^2 - \frac{1}{4}(F'_{\mu\nu})^2 - \frac{\epsilon}{2}F^{\mu\nu}F'_{\mu\nu} + \frac{1}{2}m_{A'}^2(A'_\mu)^2, \quad (1)$$

where ϵ is the dimensionless kinetic mixing parameter, and $m_{A'}$ is the A' mass. F and F' are the field strength tensors for γ and A' , respectively. For A' DM in the range 10^{-15} – 10^{-11} eV, which is of interest in this Letter, astrophysical and cosmological probes set a limit of $\epsilon \lesssim 10^{-13}$. We refer the reader to Fig. 1 of Ref. [69] for a review of these limits.

The presence of kinetic mixing, and the resulting mismatch between the interaction and propagation eigenstates, induce oscillations of dark photons into photons, $A' \rightarrow \gamma$, and vice versa. In the presence of a plasma, ordinary photons acquire an effective mass, m_γ , given primarily by the plasma frequency of the medium [31,70,71]. At every point in space \vec{x} and redshift z , the effective plasma mass is given by

$$m_\gamma^2(z, \vec{x}) \simeq 1.4 \times 10^{-21} \text{ eV}^2 c^{-4} \left(\frac{n_e(z, \vec{x})}{\text{cm}^{-3}} \right), \quad (2)$$

where n_e is the free-electron number density.

At points in space where $m_\gamma^2(z, \vec{x}) = m_{A'}^2$, the probability of conversion is resonantly enhanced [30,31,70,71]. This process can be understood as a two-level quantum system with an energy difference that is initially well separated, but with one state having its energy evolve with time. Whenever the energy difference passes through zero, a nonadiabatic transition between the two states occurs, with transition probability described by the Landau-Zener formula [31,70,72,73].

If A' constitutes the DM, the probability of conversion of A' into photons is [29–31]

$$P_{A' \rightarrow \gamma}(\vec{x}, t_{\text{res}}) \simeq \pi \epsilon^2 \frac{m_{A'} c^2}{\hbar} \left| \frac{d \ln m_\gamma^2(\vec{x}, t)}{dt} \right|_{t=t_{\text{res}}}^{-1}, \quad (3)$$

where t_{res} is the time at which the resonant condition is met. Here, $h_p \equiv 2\pi\hbar$ is Planck's constant.

For $m_{A'}$ between 10^{-15} – 10^{-12} eV c^{-2} , A' DM converts into low-frequency photons with frequency $\nu = m_{A'} c^2 / h_p$, which rapidly undergo free-free absorption in the ionized IGM. The mean free path, λ_{ff} , is given approximately by [74,75]

$$\lambda_{\text{ff}}^{-1} \simeq \frac{\alpha \sigma_T n_e^2}{2\pi \sqrt{6\pi}} \left(\frac{h_p}{m_e c} \right)^3 \left(\frac{k_B T}{h_p \nu} \right)^2 \left(\frac{m_e c^2}{k_B T} \right)^{7/2} g_{\text{ff}}(\nu, T), \quad (4)$$

where $\alpha \simeq 1/137$ is the fine-structure constant, σ_T is the Thomson cross section, T is the temperature of the IGM, and $g_{\text{ff}}(\nu, T)$ is the Gaunt factor, which only has a mild dependence on ν and T . To obtain numerical estimates, we make two simplifying approximations: (i) the Universe is completely ionized, and (ii) the local overdensities of any given cosmological species, defined as $\Delta_i \equiv \rho_i / \langle \rho_i \rangle$, where ρ_i and $\langle \rho_i \rangle$ are the local and mean energy density of species i , are all equal. Under these assumptions, $\Delta_e = \Delta_b$ and $n_e \propto (1+z)^3 \Delta_b$, where b stands for baryons. Numerically, taking $g_{\text{ff}} = 15.7$ [76], we find

$$\lambda_{\text{ff}} \sim \frac{14 \text{ kpc}}{(1+z)^6} \Delta_b^{-2} \left(\frac{T}{10^4 \text{ K}} \right)^{3/2} \left(\frac{m_{A'}}{10^{-13} \text{ eV} c^{-2}} \right)^2, \quad (5)$$

in proper units. Since Eq. (5) shows that λ_{ff} is much smaller than the typical size of a Ly- α forest absorber (~ 100 kpc), we can safely assume that the absorption of these photons occurs locally in our simulations.

Since $A' \rightarrow \gamma$ conversions only occur when the resonance condition is met, at each point in time, heating only takes place in regions of specific Δ_b , such that $m_\gamma^2(z, \vec{x}) = m_{A'}^2$ is satisfied. Moreover, the probability of conversion is governed by the rate at which Δ_b is evolving in each of

those regions. In regions where conversions are happening, the energy deposited per baryon $E_{A' \rightarrow \gamma}$ due to such a resonance is simply $E_{A' \rightarrow \gamma} = (\rho_{A'} c^2 / n_b) P_{A' \rightarrow \gamma}$, where n_b is the local number density of baryons, and $\rho_{A'}$ is the mass density of A' DM.

We can estimate $E_{A' \rightarrow \gamma}$ given our simplifying assumption of $n_e \propto (1+z)^3 \Delta_b$. Under this simplification, $|dn_{\gamma}/dt| = 3H(z)$, where $H(z)$ is the Hubble parameter, and the probability of conversion simplifies to $P_{A' \rightarrow \gamma} = \pi \epsilon^2 m_{A'} c^2 / [3H(z_{\text{res}}) \hbar]$, with z_{res} indicating the redshift at which the resonance condition is met. For $m_{A'} \sim 8 \times 10^{-14} \text{ eV} c^{-2}$, we expect baryons at the mean cosmological density to experience resonant conversion at $z \sim 2$. Therefore, the energy injected simply reads

$$E_{A' \rightarrow \gamma} = \frac{\rho_{A'} c^2}{n_b} P_{A' \rightarrow \gamma} \sim \frac{\rho_{A'} c^2}{n_b} \frac{\pi \epsilon^2 m_{A'} c^2}{3H(z_{\text{res}}) \hbar}. \quad (6)$$

Further assuming matter domination so that $H(z) \propto (1+z)^{3/2}$, and $\Delta_{\text{dm}} = \Delta_b$, we obtain approximately

$$E_{A' \rightarrow \gamma} \sim 2.5 \text{ eV} \left(\frac{\epsilon_{-14}}{0.5} \right)^2 \left(\frac{3}{1+z_{\text{res}}} \right)^{3/2} \left(\frac{m_{-13}}{0.8} \right), \quad (7)$$

where $\epsilon_{-14} \equiv \epsilon/10^{-14}$, and $m_{-13} \equiv m_{A'}/(10^{-13} \text{ eV} c^{-2})$. We see that even a mixing as small as $\epsilon_{-14} \sim 1$ leads to the absorption of enough photons to heat the IGM by several eV per baryon [29–32].

The resonant nature of A' heating makes it an attractive model for reconciling low and high redshift Ly- α forest data. The smaller the value of $m_{A'}$, the later the resonance condition is met at fixed Δ_b . For a sufficiently light A' , most of the resonant conversions occur at $z \lesssim 2$, broadening the absorption line widths at low redshifts, without depositing a significant amount of heat at $z > 2$. Furthermore, the resonance condition is set by $n_e \propto (1+z)^3 \Delta_b$, since the plasma mass tracks the electron density as shown in Eq. (2), implying that $(1+z_{\text{res}}) \propto \Delta_b^{-1/3}$ and $E_{A' \rightarrow \gamma} \propto \Delta_b^{1/2}$ during matter domination. This gives approximately the density dependence required by observations [47].

Simulations.—To fully test the viability of heating from A' DM, we now turn to implementing this model in Ly- α forest simulations for the first time. Cosmological hydrodynamical simulations of the Ly- α forest were performed with a version of P-Gadget-3 [77], modified for the Sherwood simulation project [14]. Following [47], we use a simulation box size of $L = 60h^{-1} \text{ cMpc}$ with 2×768^3 gas and DM particles, giving a gas (DM) particle mass of $M_{\text{gas}} = 6.38 \times 10^6 h^{-1} M_{\odot}$ ($M_{\text{dm}} = 3.44 \times 10^7 h^{-1} M_{\odot}$). The simulations were started at $z = 99$, with initial conditions generated on a regular grid using a Λ CDM transfer function generated by CAMB [78]. The cosmological parameters we use are $\Omega_m = 0.308$, $\Omega_{\Lambda} = 0.692$, $h = 0.678$, $\Omega_b = 0.0482$, $\sigma_8 = 0.829$, and $n = 0.961$ [79], with a

primordial helium fraction by mass of $Y_p = 0.24$. All gas particles with overdensity $\Delta_b > 10^3$ and temperature $T < 10^5 \text{ K}$ are converted into collisionless star particles, and photoionization and heating by a spatially uniform UV background is included [13]. Mock Ly- α forest spectra were extracted from the simulations and processed to resemble COS observational data following the approach described by [47], where further details and tests of our numerical methodology can be found.

In contrast to [47], however, in this Letter we also implement dark photon heating in our hydrodynamical simulations using Eq. (6). It will be numerically convenient to assume the baryons closely trace the DM in the IGM, and indeed, on scales exceeding $\sim 100 \text{ kpc}$ (the pressure smoothing scale in the IGM), this is a good approximation. We thus assume $\Delta_{\text{dm}} = \Delta_b = \rho_b / \langle \rho_b \rangle$ for $\langle \rho_b \rangle = \rho_{\text{crit}} \Omega_b (1+z)^3$, where $\rho_b \equiv \rho_b(\vec{x}, z)$ is determined for each gas particle at position \vec{x} and redshift z in our simulations. For each gas particle, we then set $\rho_{A'}(\vec{x}, z) = \Delta_b(\vec{x}, z) \rho_{\text{crit}} (\Omega_m - \Omega_b) \times (1+z)^3$. For a fixed value of $m_{A'}$, we may therefore determine where and when a resonant conversion happens for each gas particle [i.e., when the condition $m_{\gamma}^2(\vec{x}, z_{\text{res}}(\vec{x})) = m_{A'}^2$ is met]. The converted energy per baryon $E_{A' \rightarrow \gamma}$ is then calculated using Eq. (3), and directly injected into the gas particles.

Results.—We first demonstrate the effect that dark photons have on the IGM temperature by considering the redshift evolution of gas parcels at fixed overdensity, Δ_b , heated by both the UV background and $E_{A' \rightarrow \gamma}$. We adapt the nonequilibrium ionization and heating calculations performed by [47] for this purpose. In the upper panels of Fig. 1 we show the thermal history of gas at the mean density, $\Delta_b = 1$. The solid gray curves correspond to UV heating only (i.e., no A'), following the synthesis model presented in [13]. The data points are IGM temperature measurements at the mean density derived from the Ly- α forest [38,41]. All other curves in Fig. 1 include A' heating. These exhibit a sharp rise in the gas temperature when the resonance condition is met. In the top left panel, we have fixed the A' mass to $m_{-13} = 0.8$ and varied the kinetic mixing parameter, ϵ . In this case, the timing of the energy injection does not change, but the amplitude of the temperature peak increases with ϵ . The top right panel instead shows the results for a fixed kinetic mixing, $\epsilon_{-14} = 0.5$, for different A' masses. In this case, smaller A' masses result in later injection of heat into the gas parcel. From this, we may already conclude that A' masses with $m_{-13} \gtrsim 0.9$ and $\epsilon_{-14} = 0.5$ are excluded by the data from [38,41] at $2 < z < 4$. This is consistent with the bounds derived analytically in [30] using earlier measurements of the mean density IGM temperature (see their Fig. 9, as well as [29,32]).

The lower panel of Fig. 1 shows the gas thermal evolution for a fixed pair of parameters [m_{-13}, ϵ_{-14}] = [0.8, 0.5], but now for varying gas overdensities. For the

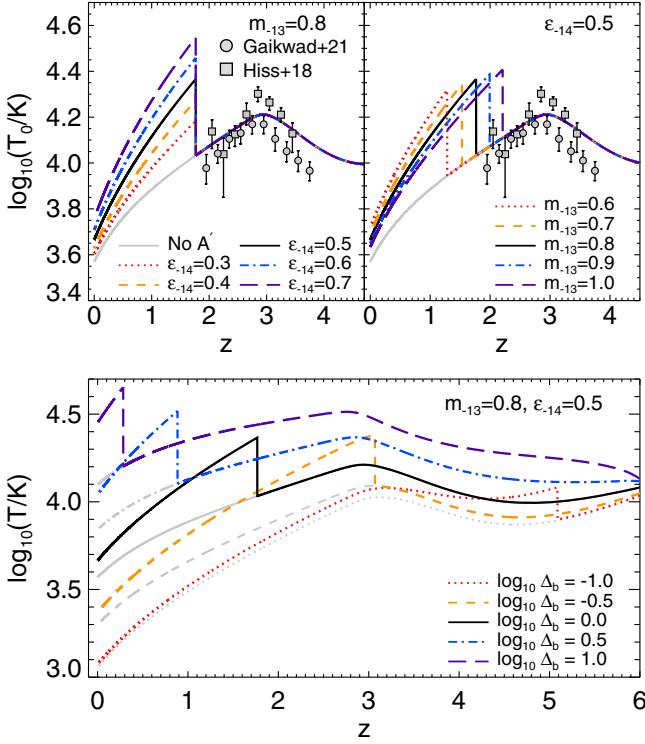


FIG. 1. Upper panels: Thermal histories for baryons at the mean background density, $\Delta_b = \rho_b / \langle \rho_b \rangle = 1$. Data points show the IGM temperature measurements from [38,41]. The gray solid curves show the case for no dark photon heating, while the other curves illustrate the effect of varying ϵ (left) or $m_{A'}$ (right). Lower panel: Thermal histories for baryons at fixed overdensities, Δ_b , assuming $m_{-13} = 0.8$ and $\epsilon_{-14} = 0.5$. Gray curves again show the case for no dark photon heating.

adopted value of the A' mass, $m_{-13} = 0.8$, the resonance at the mean background density occurs at $z_{\text{res}} = 1.8$ (black solid curve). Later energy injection occurs for overdensities ($\log_{10} \Delta_b > 0$), while earlier energy injection occurs for underdensities ($\log_{10} \Delta_b < 0$). This density dependence allows low-redshift Ly- α forest observations to place a bound on A' heating that is complementary to constraints obtained at $z > 2$. The Ly- α forest at $z = 0.1$ is sensitive to gas at overdensities of $\Delta_b \simeq 10$ [47], whereas at $z > 2$, it probes gas close to the mean density [36]. Hence, if appealing to A' heating as a possible resolution to the COS linewidth discrepancy, we require $m_{-13} > 0.6$ for resonant conversion to occur in gas with $\Delta_b = 10$ by $z = 0.1$; smaller masses would inject the energy too late. Coupled with the upper bound from data at $2 < z < 4$, this implies $0.6 \lesssim m_{-13} \lesssim 0.9$ for all kinetic mixing parameters that heat the IGM by more than a few thousand degrees. Note also that heating of the *underdense* IGM is expected at $z > 2$, even if the mean density IGM temperature constraints at $2 < z < 4$ are fully satisfied. Intriguingly, there are indeed hints from the distribution of the Ly- α forest transmitted flux that underdense gas in the IGM at $z = 3$ is hotter than expected in canonical UV

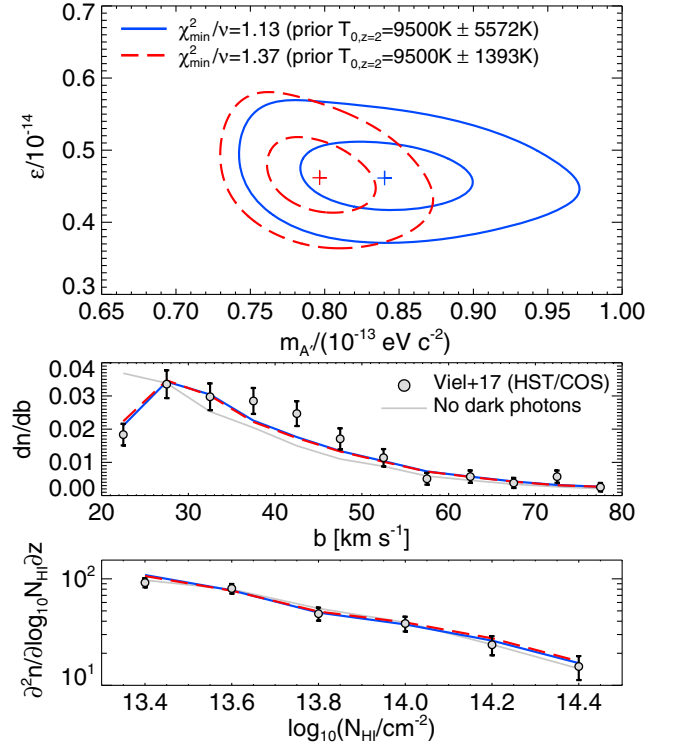


FIG. 2. Upper panel: Fit to the b -parameter distribution and CDDF of the Ly- α forest at $z = 0.1$ [42,46] assuming a *maximal* contribution of dark photon heating to the linewidths. Contours show $\Delta\chi^2 = \chi^2 - \chi_{\text{min}}^2 = 1$ and 4, corresponding to the projection of the 68% and 95% intervals for the individual parameters $m_{A'}$ and ϵ . The dashed red curves show the results for a tight prior on the $z = 2$ IGM temperature at mean density from [41]. The solid blue curves show the effect of a weaker prior, where the 1σ uncertainty from [41] has been increased by a factor of 4 for consistency with the independent temperature measurement from [38]. Lower panels: The corresponding best-fit models compared to the COS observational data. The solid gray curve shows the UV heating model with no dark photon heating [13].

photoheating models [80,81]. We intend to explore this further in future Letter.

We now turn to obtaining a best-fit dark photon dark matter model from the low-redshift Ly- α forest assuming *maximal* A' heating, i.e., with no other sources of non-canonical heating. Using the recipe outlined in the previous section, we have performed nine hydrodynamical simulations with different values of the A' mass, $m_{-13} = [0.6, 0.8, 1.0]$, and kinetic mixing, $\epsilon_{-14} = [0.3, 0.5, 0.7]$. Voigt profiles were fit to the mock Ly- α spectra, giving the Ly- α line column densities, N_{HI} , and Doppler parameters, b . The b distribution and column density distribution function (CDDF) were then constructed for each simulation following [47], and the model grid was used to perform a χ^2 minimization on the covariance matrix derived from the COS observations.

The resulting best fit A' parameters are presented in Fig. 2. The $\Delta\chi^2 = \chi^2 - \chi_{\text{min}}^2$ contours corresponding to the

68% and 95% intervals for individual parameters are displayed in the upper panel, while the lower panels show the best-fit models (corresponding to the crosses in the upper panel). We assume two different priors on the temperature of the IGM at $z = 2$: a tight prior of $T_{0,z=2} = 9500 \pm 1393$ K based on [41] (red dashed contours), and a weaker prior where the 1σ uncertainty on $T_{0,z=2}$ has been increased by a factor of 4 for consistency with the independent measurement of $T_{0,z=2} = 13721^{+1694}_{-2152}$ K from [38] (blue solid contours). As expected from Fig. 1, a weaker prior has the effect of increasing the best-fit A' mass. For the weak (tight) $z = 2$ prior, the best-fit model has $m_{-13} = 0.84 \pm 0.06$ ($m_{-13} = 0.80 \pm 0.04$) and $\epsilon_{-14} = 0.46^{+0.05}_{-0.04}$ ($\epsilon_{-14} = 0.46^{+0.06}_{-0.05}$) (1σ) for $\chi^2_{\min}/\nu = 1.13$ ($\chi^2_{\min}/\nu = 1.37$) and $\nu = 16$ degrees of freedom, with a p value of $p = 0.32$ ($p = 0.14$). For comparison, a model with UV photon heating only [13], shown by the gray curves in the lower panels of Fig. 2, has $\chi^2_{\min}/\nu = 3.50$ and $p = 2.5 \times 10^{-6}$ assuming the weak $z = 2$ thermal prior. The addition of A' heating considerably improves the fit and leads to very good agreement with the COS data. For the weak $z = 2$ prior, the best-fit A' parameters deposit an extra 5.3 eV per baryon into gas with $\Delta_b = 10$ by $z = 0.1$, consistent with the limit of $\lesssim 6.9$ eV per baryon obtained by [47].

Conclusions.—In this Letter we have pioneered the use of the Ly- α forest at redshift $z \simeq 0.1$ as a calorimeter for investigating properties of the dark sector. Specifically, we studied a model of ultralight dark photons, A' , that can naturally alleviate the tension [42–44,47] between the (too narrow) Ly- α absorption linewidths predicted in hydrodynamical simulations compared to observational data at $z = 0.1$. Assuming a *maximal* contribution from A' heating and a thermal prior of $T_0 = 9500 \pm 5572$ K at $z = 2$ [38,41], our best-fit model has A' mass $m_{A'} = 8.4 \pm 0.6 \times 10^{-14}$ eVc $^{-2}$ and kinetic mixing parameter $\epsilon = 4.6^{+0.5}_{-0.4} \times 10^{-15}$ (1σ). Although astrophysical sources, such as turbulent broadening or other non-canonical heating processes may also explain the linewidth discrepancy, our study is a first clear indication that DM energy injection can be a compelling alternative. We also highlight that our best-fit A' parameters will have testable consequences for the temperature of the underdense IGM at $z = 3$, where there are already hints of missing heating in Ly- α forest simulations [80,81], due to the unique density dependence of heating shown in Fig. 1. This temperature-density relation is a powerful test of this model, and will be explored in future Letter. More generally, our study demonstrates that a detailed study of the properties of the IGM and its observables can place stringent bounds on well-motivated dark sector models like A' DM.

Finally, we note that dark photons in our mass range of interest can be produced around spinning black holes (BHs) through the superradiance instability. The superradiant

cloud can affect the spin-mass distribution of BHs or produce gravitational waves, giving a promising way to look for A' with $m_{A'} \sim 8 \times 10^{-14}$ eVc $^{-2}$. At the moment, BH measurements appear to be in tension with this A' mass [82–84], but are currently subject to significant uncertainties [84,85] and model dependence [82,86–88]. Sharpening our understanding of the superradiance phenomenon, as well as improving the experimental searches, will be pivotal in testing our model.

A. C. is supported by the Foreign Postdoctoral Fellowship Program of the Israel Academy of Sciences and Humanities and also acknowledges support from the Israel Science Foundation (Grant 1302/19) and the European Research Council (ERC) under the EU Horizon 2020 Programme (ERC-CoG-2015-Proposal No. 682676 LDMThExp). H. L. is supported by NSF Grant No. PHY-1915409, the DOE under Award No. DE-SC0007968 and the Simons Foundation. M. V. is supported by the PD51-INFN INDARK and ASI-INAF n. 2017-14-H.0 grants. J. S. B. is supported by Science and Technology Facilities Council (STFC) consolidated grant ST/T000171/1. The hydrodynamical simulations were performed using the DiRAC@Durham facility managed by the Institute for Computational Cosmology on behalf of the STFC DiRAC HPC Facility. The equipment was funded by BEIS capital funding via STFC capital grants ST/P002293/1 and ST/R002371/1, Durham University and STFC operations Grant No. ST/R000832/1.

*james.bolton@nottingham.ac.uk

†andreacaputo@mail.tau.ac.il

‡hongwanl@princeton.edu

§viel@sissa.it

- [1] M. McQuinn, The evolution of the intergalactic medium, *Annu. Rev. Astron. Astrophys.* **54**, 313 (2016).
- [2] M. Viel, J. Lesgourgues, M. G. Haehnelt, S. Matarrese, and A. Riotto, Constraining warm dark matter candidates including sterile neutrinos and light gravitinos with WMAP and the Lyman-alpha forest, *Phys. Rev. D* **71**, 063534 (2005).
- [3] A. Boyarsky, J. Lesgourgues, O. Ruchayskiy, and M. Viel, Lyman-alpha constraints on warm and on warm-plus-cold dark matter models, *J. Cosmol. Astropart. Phys.* **05** (2009) 012.
- [4] M. Viel, G. D. Becker, J. S. Bolton, and M. G. Haehnelt, Warm dark matter as a solution to the small scale crisis: New constraints from high redshift Lyman- α forest data, *Phys. Rev. D* **88**, 043502 (2013).
- [5] N. Palanque-Delabrouille, C. Yèche, N. Schöneberg, J. Lesgourgues, M. Walther, S. Chabanier, and E. Armengaud, Hints, neutrino bounds, and WDM constraints from SDSS DR14 Lyman- α and Planck full-survey data, *J. Cosmol. Astropart. Phys.* **04** (2020) 038.
- [6] V. K. Narayanan, D. N. Spergel, R. Dave, and C.-P. Ma, Constraints on the mass of warm dark matter particles and

- the shape of the linear power spectrum from the Ly α forest, *Astrophys. J. Lett.* **543**, L103 (2000).
- [7] V. Iršič, M. Viel, M. G. Haehnelt, J. S. Bolton, and G. D. Becker, First Constraints on Fuzzy Dark Matter from Lyman- α Forest Data and Hydrodynamical Simulations, *Phys. Rev. Lett.* **119**, 031302 (2017).
- [8] T. Kobayashi, R. Murgia, A. De Simone, V. Iršič, and M. Viel, Lyman- α constraints on ultralight scalar dark matter: Implications for the early and late universe, *Phys. Rev. D* **96**, 123514 (2017).
- [9] E. Armengaud, N. Palanque-Delabrouille, C. Yèche, D. J. E. Marsh, and J. Baur, Constraining the mass of light bosonic dark matter using SDSS Lyman- α forest, *Mon. Not. R. Astron. Soc.* **471**, 4606 (2017).
- [10] K. K. Rogers and H. V. Peiris, Strong Bound on Canonical Ultralight Axion Dark Matter from the Lyman-Alpha Forest, *Phys. Rev. Lett.* **126**, 071302 (2021).
- [11] R. Murgia, G. Scelfo, M. Viel, and A. Raccanelli, Lyman- α Forest Constraints on Primordial Black Holes as Dark Matter, *Phys. Rev. Lett.* **123**, 071102 (2019).
- [12] J. Miralda-Escudé and M. J. Rees, Reionization and thermal evolution of a photoionized intergalactic medium, *Mon. Not. R. Astron. Soc.* **266**, 343 (1994).
- [13] E. Puchwein, F. Haardt, M. G. Haehnelt, and P. Madau, Consistent modelling of the meta-galactic UV background and the thermal/ionization history of the intergalactic medium, *Mon. Not. R. Astron. Soc.* **485**, 47 (2019).
- [14] J. S. Bolton, E. Puchwein, D. Sijacki, M. G. Haehnelt, T.-S. Kim, A. Meiksin, J. A. Regan, and M. Viel, The Sherwood simulation suite: Overview and data comparisons with the Lyman α forest at redshifts $2 \leq z \leq 5$, *Mon. Not. R. Astron. Soc.* **464**, 897 (2017).
- [15] B. Villaseñor, B. Robertson, P. Madau, and E. Schneider, Inferring the thermal history of the intergalactic medium from the properties of the hydrogen and helium Lyman-alpha forest, *Astrophys. J.* **933**, 59 (2022).
- [16] M. Cirelli, F. Iocco, and P. Panci, Constraints on dark matter annihilations from reionization and heating of the intergalactic gas, *J. Cosmol. Astropart. Phys.* **10** (2009) 009.
- [17] R. Diamanti, L. Lopez-Honorez, O. Mena, S. Palomares-Ruiz, and A. C. Vincent, Constraining dark matter late-time energy injection: Decays and P-wave annihilations, *J. Cosmol. Astropart. Phys.* **02** (2014) 017.
- [18] H. Liu, T. R. Slatyer, and J. Zavala, Contributions to cosmic reionization from dark matter annihilation and decay, *Phys. Rev. D* **94**, 063507 (2016).
- [19] C. Evoli, A. Mesinger, and A. Ferrara, Unveiling the nature of dark matter with high redshift 21 cm line experiments, *J. Cosmol. Astropart. Phys.* **11** (2014) 024.
- [20] L. Lopez-Honorez, O. Mena, A. Moliné, S. Palomares-Ruiz, and A. C. Vincent, The 21 cm signal and the interplay between dark matter annihilations and astrophysical processes, *J. Cosmol. Astropart. Phys.* **08** (2016) 004.
- [21] G. D'Amico, P. Panci, and A. Strumia, Bounds on Dark Matter Annihilations from 21 cm Data, *Phys. Rev. Lett.* **121**, 011103 (2018).
- [22] H. Liu and T. R. Slatyer, Implications of a 21-cm signal for dark matter annihilation and decay, *Phys. Rev. D* **98**, 023501 (2018).
- [23] K. Cheung, J.-L. Kuo, K.-W. Ng, and Y.-L. S. Tsai, The impact of EDGES 21-cm data on dark matter interactions, *Phys. Lett. B* **789**, 137 (2019).
- [24] A. Mitridate and A. Podo, Bounds on dark matter decay from 21 cm line, *J. Cosmol. Astropart. Phys.* **05** (2018) 069.
- [25] S. Clark, B. Dutta, Y. Gao, Y.-Z. Ma, and L. E. Strigari, 21 cm limits on decaying dark matter and primordial black holes, *Phys. Rev. D* **98**, 043006 (2018).
- [26] H. Liu, W. Qin, G. W. Ridgway, and T. R. Slatyer, Lyman- α constraints on cosmic heating from dark matter annihilation and decay, *Phys. Rev. D* **104**, 043514 (2021).
- [27] B. S. Haridasu and M. Viel, Late-time decaying dark matter: constraints and implications for the H_0 -tension, *Mon. Not. R. Astron. Soc.* **497**, 1757 (2020).
- [28] J. B. Muñoz and A. Loeb, Constraints on dark matter-baryon scattering from the temperature evolution of the intergalactic medium, *J. Cosmol. Astropart. Phys.* **11** (2017) 043.
- [29] S. D. McDermott and S. J. Witte, Cosmological evolution of light dark photon dark matter, *Phys. Rev. D* **101**, 063030 (2020).
- [30] A. Caputo, H. Liu, S. Mishra-Sharma, and J. T. Ruderman, Dark Photon Oscillations in Our Inhomogeneous Universe, *Phys. Rev. Lett.* **125**, 221303 (2020).
- [31] A. Caputo, H. Liu, S. Mishra-Sharma, and J. T. Ruderman, Modeling dark photon oscillations in our inhomogeneous universe, *Phys. Rev. D* **102**, 103533 (2020).
- [32] S. J. Witte, S. Roscauro-Alcaraz, S. D. McDermott, and V. Poulin, Dark photon dark matter in the presence of inhomogeneous structure, *J. High Energy Phys.* **06** (2020) 132.
- [33] J. Schaye, T. Theuns, M. Rauch, G. Efstathiou, and W. L. W. Sargent, The thermal history of the intergalactic medium*, *Mon. Not. R. Astron. Soc.* **318**, 817 (2000).
- [34] M. Ricotti, N. Y. Gnedin, and J. M. Shull, The evolution of the effective equation of state of the intergalactic medium, *Astrophys. J.* **534**, 41 (2000).
- [35] A. Lidz, C.-A. Faucher-Giguère, A. Dall'Aglio, M. McQuinn, C. Fechner, M. Zaldarriaga, L. Hernquist, and S. Dutta, A measurement of small-scale structure in the $2.2 \leq z \leq 4.2$ Ly α forest, *Astrophys. J.* **718**, 199 (2010).
- [36] G. D. Becker, J. S. Bolton, M. G. Haehnelt, and W. L. W. Sargent, Detection of extended He II reionization in the temperature evolution of the intergalactic medium, *Mon. Not. R. Astron. Soc.* **410**, 1096 (2011).
- [37] E. Boera, M. T. Murphy, G. D. Becker, and J. S. Bolton, The thermal history of the intergalactic medium down to redshift $z = 1.5$: A new curvature measurement, *Mon. Not. R. Astron. Soc.* **441**, 1916 (2014).
- [38] H. Hiss, M. Walther, J. F. Hennawi, J. Oñorbe, J. M. O'Meara, A. Rorai, and Z. Lukić, A new measurement of the temperature-density relation of the IGM from Voigt profile fitting, *Astrophys. J.* **865**, 42 (2018).
- [39] M. Walther, J. Oñorbe, J. F. Hennawi, and Z. Lukić, New constraints on IGM thermal evolution from the Ly α forest power spectrum, *Astrophys. J.* **872**, 13 (2019).
- [40] K. N. Telikova, P. S. Shternin, and S. A. Balashev, Thermal state of the intergalactic medium at $z \sim 2-4$, *Astrophys. J.* **887**, 205 (2019).
- [41] P. Gaikwad, R. Srianand, M. G. Haehnelt, and T. R. Choudhury, A consistent and robust measurement of the

- thermal state of the IGM at $2 \leq z \leq 4$ from a large sample of Ly α forest spectra: Evidence for late and rapid He II reionization, *Mon. Not. R. Astron. Soc.* **506**, 4389 (2021).
- [42] M. Viel, M. G. Haehnelt, J. S. Bolton, T.-S. Kim, E. Puchwein, F. Nasir, and B. P. Wakker, Diagnosing galactic feedback with line broadening in the low-redshift Ly α forest, *Mon. Not. R. Astron. Soc.* **467**, L86 (2017).
- [43] P. Gaikwad, R. Srianand, T. R. Choudhury, and V. Khair, VoIgt profile Parameter Estimation Routine (VIPER): H I photoionization rate at $z < 0.5$, *Mon. Not. R. Astron. Soc.* **467**, 3172 (2017).
- [44] B. Burkhart, M. Tillman, A. B. Gurvich, S. Bird, S. Tonnesen, G. L. Bryan, L. E. Hernquist, and R. S. Somerville, The low redshift Lyman- α forest as a constraint for models of AGN feedback, *Astrophys. J. Lett.* **933**, L46 (2022).
- [45] C. W. Danforth, B. A. Keeney, E. M. Tilton, J. M. Shull, J. T. Stocke, M. Stevans, M. M. Pieri, B. D. Savage, K. France, D. Syphers, B. D. Smith, J. C. Green, C. Froning, S. V. Penton, and S. N. Osterman, An HST/COS survey of the low-redshift intergalactic medium. I. Survey, methodology, and overall results, *Astrophys. J.* **817**, 111 (2016).
- [46] T. S. Kim, B. P. Wakker, F. Nasir, R. F. Carswell, B. D. Savage, J. S. Bolton, A. J. Fox, M. Viel, M. G. Haehnelt, J. C. Charlton, and B. E. Rosenwasser, The evolution of the low-density HI intergalactic medium from $z = 3.6$ to 0: Data, transmitted flux, and HI column density, *Mon. Not. R. Astron. Soc.* **501**, 5811 (2021).
- [47] J. S. Bolton, P. Gaikwad, M. G. Haehnelt, T.-S. Kim, F. Nasir, E. Puchwein, M. Viel, and B. P. Wakker, Limits on non-canonical heating and turbulence in the intergalactic medium from the low redshift Lyman α forest, *Mon. Not. R. Astron. Soc.* **513**, 864 (2022).
- [48] C. Evoli and A. Ferrara, Turbulence in the intergalactic medium, *Mon. Not. R. Astron. Soc.* **413**, 2721 (2011).
- [49] L. Iapichino, M. Viel, and S. Borgani, Turbulence driven by structure formation in the circumgalactic medium, *Mon. Not. R. Astron. Soc.* **432**, 2529 (2013).
- [50] B. Holdom, Two U(1)'s and epsilon charge shifts, *Phys. Lett.* **166B**, 196 (1986).
- [51] K. R. Dienes, C. F. Kolda, and J. March-Russell, Kinetic mixing and the supersymmetric gauge hierarchy, *Nucl. Phys.* **B492**, 104 (1997).
- [52] M. Goodsell, J. Jaeckel, J. Redondo, and A. Ringwald, Naturally light hidden photons in LARGE volume string compactifications, *J. High Energy Phys.* **11** (2009) 027.
- [53] M. Goodsell and A. Ringwald, Light hidden-sector U(1)s in string compactifications, *Fortschr. Phys.* **58**, 716 (2010).
- [54] M. Goodsell, Light hidden U(1)s from string theory, in *Proceedings of the 5th Patras Workshop on Axions, WIMPs and WISPs* (DESY, Hamburg, 2010), pp. 165–168.
- [55] S. A. Abel and B. W. Schofield, Brane anti-brane kinetic mixing, millicharged particles and SUSY breaking, *Nucl. Phys.* **B685**, 150 (2004).
- [56] S. A. Abel, J. Jaeckel, V. V. Khoze, and A. Ringwald, Illuminating the hidden sector of string theory by shining light through a magnetic field, *Phys. Lett. B* **666**, 66 (2008).
- [57] S. A. Abel, M. D. Goodsell, J. Jaeckel, V. V. Khoze, and A. Ringwald, Kinetic mixing of the photon with hidden U(1)s in string phenomenology, *J. High Energy Phys.* **07** (2008) 124.
- [58] J. Redondo and M. Postma, Massive hidden photons as lukewarm dark matter, *J. Cosmol. Astropart. Phys.* **02** (2009) 005.
- [59] A. E. Nelson and J. Scholtz, Dark light, dark matter and the misalignment mechanism, *Phys. Rev. D* **84**, 103501 (2011).
- [60] P. Arias, D. Cadamuro, M. Goodsell, J. Jaeckel, J. Redondo, and A. Ringwald, WISPy cold dark matter, *J. Cosmol. Astropart. Phys.* **06** (2012) 013.
- [61] A. Fradette, M. Pospelov, J. Pradler, and A. Ritz, Cosmological constraints on very dark photons, *Phys. Rev. D* **90**, 035022 (2014).
- [62] H. An, M. Pospelov, J. Pradler, and A. Ritz, Direct detection constraints on dark photon dark matter, *Phys. Lett. B* **747**, 331 (2015).
- [63] P. W. Graham, J. Mardon, and S. Rajendran, Vector dark matter from inflationary fluctuations, *Phys. Rev. D* **93**, 103520 (2016).
- [64] P. Agrawal, N. Kitajima, M. Reece, T. Sekiguchi, and F. Takahashi, Relic abundance of dark photon dark matter, *Phys. Lett. B* **801**, 135136 (2020).
- [65] J. A. Dror, K. Harigaya, and V. Narayan, Parametric resonance production of ultralight vector dark matter, *Phys. Rev. D* **99**, 035036 (2019).
- [66] R. T. Co, A. Pierce, Z. Zhang, and Y. Zhao, Dark photon dark matter produced by axion oscillations, *Phys. Rev. D* **99**, 075002 (2019).
- [67] M. Bastero-Gil, J. Santiago, L. Ubaldi, and R. Vega-Morales, Vector dark matter production at the end of inflation, *J. Cosmol. Astropart. Phys.* **04** (2019) 015.
- [68] A. J. Long and L.-T. Wang, Dark photon dark matter from a network of cosmic strings, *Phys. Rev. D* **99**, 063529 (2019).
- [69] A. Caputo, A. J. Millar, C. A. J. O'Hare, and E. Vitagliano, Dark photon limits: A handbook, *Phys. Rev. D* **104**, 095029 (2021).
- [70] A. Mirizzi, J. Redondo, and G. Sigl, Microwave background constraints on mixing of photons with hidden photons, *J. Cosmol. Astropart. Phys.* **03** (2009) 026.
- [71] K. E. Kunze and M. Á. Vázquez-Mozo, Constraints on hidden photons from current and future observations of CMB spectral distortions, *J. Cosmol. Astropart. Phys.* **12** (2015) 028.
- [72] S. J. Parke, Nonadiabatic Level Crossing in Resonant Neutrino Oscillations, *Phys. Rev. Lett.* **57**, 1275 (1986).
- [73] T.-K. Kuo and J. T. Pantaleone, Neutrino oscillations in matter, *Rev. Mod. Phys.* **61**, 937 (1989).
- [74] B. T. Draine, *Physics of the Interstellar And Intergalactic Medium* (Princeton University Press, Princeton, 2011).
- [75] J. Chluba, Green's function of the cosmological thermalization problem—II. Effect of photon injection and constraints, *Mon. Not. R. Astron. Soc.* **454**, 4182 (2015).
- [76] B. C. Lacki, The end of the rainbow: What can we say about the extragalactic sub-megahertz radio sky?, *Mon. Not. R. Astron. Soc.* **406**, 863 (2010).
- [77] V. Springel, The cosmological simulation code GADGET-2, *Mon. Not. R. Astron. Soc.* **364**, 1105 (2005).
- [78] A. Lewis, A. Challinor, and A. Lasenby, Efficient computation of CMB anisotropies in closed FRW models, *Astrophys. J.* **538**, 473 (2000).

- [79] P. A. R. Ade, N. Aghanim, C. Armitage-Caplan, M. Arnaud, M. Ashdown, F. Atrio-Barandela, J. Aumont, C. Baccigalupi, A. J. Banday *et al.* (Planck Collaboration), Planck 2013 results. XVI. Cosmological parameters, *Astron. Astrophys.* **571**, A16 (2014).
- [80] J. S. Bolton, M. Viel, T. S. Kim, M. G. Haehnelt, and R. F. Carswell, Possible evidence for an inverted temperature-density relation in the intergalactic medium from the flux distribution of the Ly α forest, *Mon. Not. R. Astron. Soc.* **386**, 1131 (2008).
- [81] A. Rorai, G. D. Becker, M. G. Haehnelt, R. F. Carswell, J. S. Bolton, S. Cristiani, V. D’Odorico, G. Cupani, P. Barai, F. Calura, T. S. Kim, E. Pomante, E. Tescari, and M. Viel, Exploring the thermal state of the low-density intergalactic medium at $z = 3$ with an ultrahigh signal-to-noise QSO spectrum, *Mon. Not. R. Astron. Soc.* **466**, 2690 (2017).
- [82] M. Baryakhtar, R. Lasenby, and M. Teo, Black hole superradiance signatures of ultralight vectors, *Phys. Rev. D* **96**, 035019 (2017).
- [83] V. Cardoso, O. J. C. Dias, G. S. Hartnett, M. Middleton, P. Pani, and J. E. Santos, Constraining the mass of dark photons and axion-like particles through black-hole superradiance, *J. Cosmol. Astropart. Phys.* **03** (2018) 043.
- [84] D. Ghosh and D. Sachdeva, Constraining light dark photons from GW190517 and GW190426_152155, *Phys. Rev. D* **103**, 095028 (2021).
- [85] K. Belczynski, C. Done, and J. P. Lasota, All Apples: Comparing black holes in X-ray binaries and gravitational-wave sources, [arXiv:2111.09401](https://arxiv.org/abs/2111.09401).
- [86] H. Fukuda and K. Nakayama, Aspects of nonlinear effect on black hole superradiance, *J. High Energy Phys.* **01** (2020) 128.
- [87] A. Caputo, S. J. Witte, D. Blas, and P. Pani, Electromagnetic signatures of dark photon superradiance, *Phys. Rev. D* **104**, 043006 (2021).
- [88] E. Cannizzaro, L. Sberna, A. Caputo, and P. Pani, Dark photon superradiance quenched by dark matter, *Phys. Rev. D* **106**, 083019 (2022).